# High-Power $Yb^{3+}$-Doped Phosphate Fiber Amplifier

Yin-Wen Lee, Michel J. F. Digonnet, *Member, IEEE*, Supriyo Sinha, Karel E. Urbanek, Robert L. Byer, *Fellow, IEEE*, and Shibin Jiang

***Abstract*—We report on the development of novel high-power light sources utilizing a $Yb^{3+}$-doped phosphate fiber as the gain element. This host presents several key benefits over silica, particularly much higher $Yb_2O_3$ concentrations (up to 26 wt%), a 50% weaker stimulated Brillouin scattering (SBS) gain cross section, and the absence of observable photodarkening even at high population inversion. These properties result in a greatly increased SBS threshold compared to silica fibers, and therefore, potentially much higher output powers out of either a multimode large mode area or a single-mode fiber, which means in the latter case a higher beam quality. To quantify these predictions, we show through numerical simulations that double-clad phosphate fibers should produce as much as ∼700 W of single-frequency output power in a step index, single-mode core. As a step in this direction, we report a short phosphate fiber amplifier doped with 12 wt% $Yb_2O_3$ that emits 16 W of single-frequency single-mode output. We also describe a single-mode phosphate fiber laser with a maximum output power of 57 W. The laser slope efficiency is currently limited by the fairly high fiber loss (∼3 dB/m). Measurements indicate that 77% of this loss originates from impurity absorption, and the rest from scattering.**

***Index Terms*—Fiber lasers and amplifiers, phosphate fiber, ytterbium.**

## I. Introduction

SPECTACULAR progress has been made over the past few years in the development of laboratory and commercial high-power $Yb^{3+}$-doped silica fiber sources [1]–[4]. This achievement has required surmounting several key challenges. The first one is efficiently coupling large continuous-wave (CW) optical powers from the stacks of spatially incoherent pump diodes into the small core of the fiber where the $Yb^{3+}$ ions are confined. Coupling the pump beam into the multimode inner cladding of a double-clad fiber [5] is now the universal solution to this problem. The second challenge was, and to some degree still is, the onset of nonlinear effects in the fiber. By far, the most troublesome of these effects for a single-frequency source is stimulated Brillouin scattering (SBS). Since the SBS gain is proportional to fiber length, the first solution has been to increase the $Yb^{3+}$ concentration to reduce the length of fiber required to absorb the pump. However, in silica, the $Yb_2O_3$ concentration can only be increased so much (of the order of 1–2 wt%) before the onset of other deleterious effects such as quenching [6] and photodarkening [7]. A second, widely used solution has been multimode large-mode-area (LMA) fibers [8], in which the core size is increased (and the fiber numerical aperture (NA) correspondingly decreased) to decrease the optical intensity, and thus, increase the SBS threshold. Single transverse-mode operation is usually obtained by coiling the fiber or designing the fiber or pump geometry so that the fundamental mode is preferentially amplified. This approach has made it possible to achieve output powers as high as 2 kW of near-diffraction-limited output from an LMA fiber laser [1]. Attaining such high powers in a single-frequency output is much more challenging, because the SBS gain of a single-frequency signal is considerably higher. Nevertheless, other clever solutions have been developed, which, in conjunction with an LMA fiber, have produced high-power single-frequency outputs, including SBS thermal broadening (500 W of output power) [4], and acoustic antiguiding fibers (502 W) [3]. This last scheme is believed to be capable of ultimately producing up to ∼1 kW of single-frequency output power [3].

One major drawback of these solutions is that by making use of an LMA fiber, they compromise one of the most outstanding and beneficial properties of an optical fiber, which is its ability to carry a single transverse mode. As a consequence, most of these high-power single-frequency sources have a significantly lower mode quality ($M^2 > 1.1$ is typical) than a truly single-mode fiber source [1]–[4]. Furthermore, it has been reported that the interference of the fundamental mode with the residual weakly guided higher order modes in the fiber cores could significantly decrease their pointing stability [9]. The mode quality can, of course, always be restored to an acceptable level with a mode cleaner [10], but this additional filtering wastes power and introduces intensity noise.

An alternative approach to high power from a fiber laser that shows great promise is to use phosphate glass instead of silica as the fiber material. The primary benefit of phosphate glass is the solubility of $Yb^{3+}$ and other rare-earth (RE) ions. Furthermore, we have shown that the SBS gain coefficient of a phosphate fiber is 50% weaker than that of silica [11]. Combined, these properties imply that the fiber length requirement for a single-frequency source is reduced by about an order of magnitude, or conversely, an order of magnitude more power can be extracted from a fiber. Finally, we have also shown that phosphate fibers doped with even as much as 12 wt% of $Yb_2O_3$ exhibit no measurable photodarkening [7]. These exceptional characteristics offer the potential of single-frequency fiber amplifiers in

Manuscript received September 2, 2008; revised October 8, 2008 and October 27, 2008; accepted October 28, 2008. Current version published February 4, 2009. This work was supported by the U.S. Army Research Office under ARO Contract DAAD19-01-1-0184.

Y.-W. Lee, M. J. F. Digonnet, K. E. Urbanek, and R. L. Byer are with Edward L. Ginzton Laboratory, Stanford University, Stanford, CA 94305 USA (e-mail: leeyw@stanford.edu; silurian@stanford.edu; kurbanek@stanford.edu; byer@stanford.edu).

S. Sinha was with Stanford University, Stanford, CA 94305 USA. He is now with Raydiance, Inc., Los Altos, CA 94022 USA (e-mail: supriyo@gmail.com).

S. Jiang was with NP Photonics, Inc., Tucson, AZ 85747 USA. He is now with AdValue Photonics, Inc., Tucson, AZ 85714 USA (e-mail: sjiang@advaluephotonics.com).

Color versions of one or more of the figures in this paper are available online at http://ieeexplore.ieee.org.

Digital Object Identifier 10.1109/JSTQE.2008.2010263

the near-kilowatt (kW) range in a step-index single-mode fiber instead of an LMA fiber, which would produce much cleaner and less noisy output beams.

To approach this goal, we report in this paper our latest progress in modeling and testing high-power single-mode single-frequency phosphate fiber amplifiers. We describe in particular a 16 W device of this kind doped with one of the highest published concentrations for a $Yb^{3+}$-doped fiber (12 wt% $Yb_2O_3$) and only 74.5 cm in length. This is the first report of a watt-class $Yb^{3+}$-doped phosphate fiber master oscillator power amplifier (MOPA). We also demonstrate power scaling to nearly 60 W in a 71.6-cm $Yb^{3+}$-doped phosphate fiber laser (not single frequency). Thermal loading calculations predict that with standard cooling, this type of fiber should be capable of producing up to 700 W of single-frequency power in a step-index, single-mode core, and considerably more in a multimode LMA fiber.

## II. Material Properties of $Yb^{3+}$-Doped Phosphate Fibers

The preforms used to fabricate the fibers tested in this paper were made of alkaline-earth phosphate glasses. The glass is composed of more than 50 mol% $P_2O_5$, as well as $A1_2O_3$, BaO, ZnO, and $La_2O_3$. $Al_2O_3$ ($\sim$5 mol%) was added to ensure high mechanical strength and good chemical durability of the glass. Alkali ions and transition metals such as Fe and Cu were eliminated to further enhance the glass properties.

The upper state lifetime of the $Yb^{3+}$ ions in 12 wt% $Yb^{3+}$-doped bulk phosphate glass was measured to be 1.2 ms, which is longer than in highly doped silica glass host ($\sim$0.8 ms) due to the presence of germanium in the latter [12]. The measured fluorescence relaxation curve showed a single exponential, thus demonstrating negligible concentration quenching in spite of the extremely high $Yb^{3+}$ concentration. The same phosphate glass host doped up to 26 wt% of $Yb_2O_3$ ($\sim$15 times as much as is possible in silica without inducing quenching) but still does not exhibit notable concentration quenching, up-conversion, or crystallization [13].

For the purposes of building high-power phosphate fiber laser sources, two types of double-clad phosphate fibers were fabricated, namely, a standard one with a circular inner cladding and a fiber with a slightly eccentric core and a small air hole some distance from it. This second fiber was designed to provide mode mixing (the role of the air hole) and improved spatial overlap between the pump modes and the doped core (the reason for the eccentricity of the core). These two effects increased the pump absorption in the doped core. Both fibers had two claddings only and were unjacketed. The outer cladding is made of phosphate glass and has thermal properties superior to the polymers widely used as outer cladding in double-clad silica fibers. A photograph of the cleaved ends of each of these fibers is shown in Fig. 1.

The preforms used to draw these fibers were manufactured by the rod-in-tube technique at NP Photonics, Tuscon, AZ. This well-developed technology is commonly used for producing soft-glass fibers [14] and silica-based fibers with compound-glass core compositions [15]. The main reason is that some of the chemicals required to fabricate a phosphate fiber by a chemical vapor deposition procedure cannot be volatilized. A core glass rod and two cladding tubes were fabricated and assembled to form the fiber preform. The core rod was cored out of a larger bulk sample with a diamond-embedded core drill, and the barrel of the rod was polished. Both the inside and outside surfaces of the glass tubes for the inner and outer claddings were polished to a high surface quality. The inside diameter of the inner cladding tube was matched to the diameter of the core rod, and the inside diameter of the outer cladding tube was matched to the outer diameter of the inner cladding tube. Both core and cladding glasses were prepared carefully to ensure that their chemical and thermomechanical characteristics were compatible, especially their softening temperature and thermal expansion coefficient. The fiber was drawn in a special furnace optimized for soft nonsilica glasses at a temperature of approximately 765 °C. The drawing process for both double-clad fibers was identical, except that a slightly positive pressure was applied to produce the air hole in the air-hole fiber.

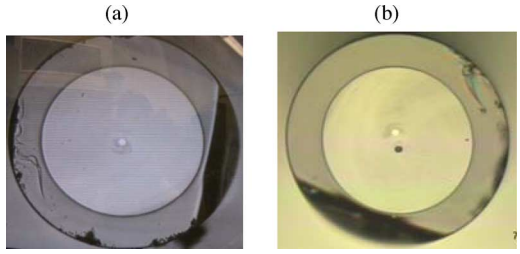


Fig. 1. Photograph of the cleaved-end face of the two types of double-clad phosphate fibers used in this paper: (a) With a concentric core. (b) With an offset core and adjacent air hole to mix the pump modes.

The propagation loss of the fundamental mode at 1310 nm was measured to be $\sim$3 dB/m in both fibers. This figure is much lower than the loss published for Er/Yb-doped phosphate fibers fabricated by a similar process [16]. The mechanisms contributing to the 3 dB/m loss are studied in Section V.

## III. Theoretical Predictions of High-Power $Yb^{3+}$-Doped Phosphate Fiber Amplifier

### A. Modeling Phosphate Fiber Laser Sources

To predict the quantitative performance of $Yb^{3+}$-doped fiber lasers and amplifiers based on phosphate and other hosts, and optimize their physical parameters, we have developed a simulation code based on the original work of Wagener *et al.* [17]. This simulator solves the coupled laser rate equations numerically to predict the output performance of the fiber source, such as the amount of pump power and the length of fiber required to achieve a certain output power level, the population inversion at every point along the fiber, the forward and backward amplified spontaneous emission (ASE) powers and spectra, the gain spectrum, excess noise, etc., in either a core-pumped or a cladding-pumped configuration. The input parameters include the fiber structure and all the relevant spectroscopic parameters, such as the ion concentration, absorption and emission cross-section spectra, and excited state lifetime. Comparison of the

code prediction to the measured properties of Er-doped superfluorescent fiber sources [18] and high-power $Yb^{3+}$-doped silica and phosphate fiber lasers [19], [20] has shown that this code is quite accurate.

### *B. 700 W Truly Single-Mode Phosphate Fiber MOPA*

To evaluate the maximum output power that can be expected from a single-frequency, truly single-mode phosphate fiber laser or amplifier before the onset of SBS, we used our code to compare the predicted performance of two fiber MOPAs, one made with a phosphate fiber and the other one with a silica fiber. For fair comparison, the two amplifiers had exactly the same fiber characteristics, and they were seeded and pumped exactly the same way. Both fibers were taken to have a step-index core diameter of 10 $\mu$m, a core NA of 0.07, and an inner cladding diameter of 125 $\mu$m. The calculated effective core area was 108 $\mu m^2$. To reflect actual differences between the two types of fibers, namely their propagation loss, upper state lifetime, and $Yb^{3+}$ concentration, each of these three parameters was given its actual measured value for each fiber. For the silica fiber, we used the best current values reported for commercial fibers, i.e., a loss of 0.03 dB/m, an upper state lifetime of 0.85 ms, and a concentration of $1.2 \times 10^{20}$ $Yb^{3+}/cm^3$ [21]. The corresponding values for the phosphate fiber were 3 dB/m, 1.2 ms, and $14.2 \times 10^{20}$ $Yb^{3+}/cm^3$, respectively. The fiber length was a free parameter. Each amplifier was seeded with 15 W of single-frequency laser light at 1064 nm and cladding-pumped 700 W in the forward direction and 300 W in the opposite direction, both at 975 nm. The pump powers were selected such that at the optimum length, the output power just reaches the damage threshold power. This imbalanced bidirectional pumping was arranged to maintain an even thermal distribution. The simulator used the actual measured absorption and emission cross-section spectra of these two fibers as input.

Fig. 2(a) and (b) shows the theoretical prediction of the output power versus fiber length for the phosphate and silica fiber MOPAs (blue solid curves), respectively. These curves were plotted for a total launched pump power of 1000 W, chosen so that the output power of the phosphate fiber MOPA is as high as possible. The maroon solid curves show the residual unabsorbed pump power. The red dashed curves represent the SBS threshold power, assuming the conventional SBS gain coefficient of $5 \times 10^{-11}$ m/W for the silica fiber and the measured value of $2.5 \times 10^{-11}$ m/W for our phosphate fiber [11].

Fig. 2 also shows the damage limitation for each fiber. The damage threshold for the silica fiber is 1.3 GW/cm$^2$ [22]. Because of the lack of experimental data, the damage threshold of phosphate fibers was taken to be 0.65 GW/cm$^2$, estimated conservatively by considering the bonding strength of P–O compared to Si–O and the measured damage threshold of Nd-doped phosphate glasses [23].

Fig. 2(a) shows that as the length of the phosphate fiber is increased, the output power first increases, then decreases, as a result of the fairly high fiber loss. The figure predicts that at its optimum length (~30 cm), the phosphate fiber MOPA will produce 702 W of single-frequency output power without

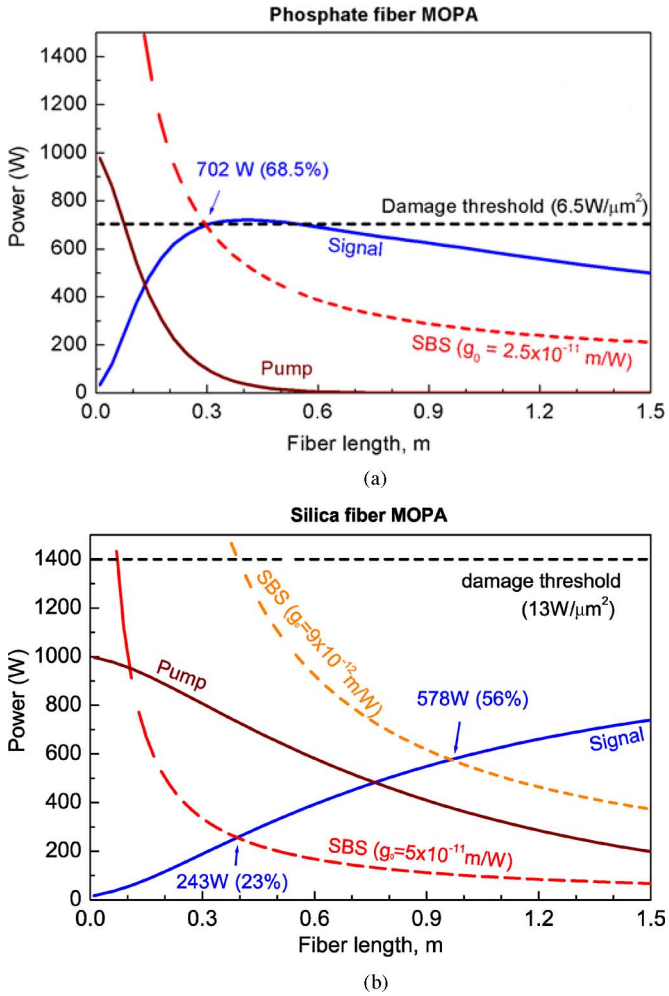


Fig. 2. Theoretical predictions of the single-frequency output power dependence on fiber length. (a) Phosphate fiber MOPA. (b) Silica fiber MOPA. The blue and maroon solid curves show the output signal and unabsorbed pump power, respectively, as a function of the fiber length. The red, orange, and black dashed curves trace the SBS and damage power thresholds, respectively.

suffering from SBS. This value is, in fact, limited not only by SBS but also by surface damage. Fig. 2(b) shows that at the same pump power level, the silica fiber MOPA produces a maximum output power of 243 W only, limited this time by the onset of SBS. Also, note that at the optimum length, most of the pump power (81%) is absorbed in the phosphate fiber MOPA, so its conversion efficiency is very high (68.5%). In contrast, in the optimized silica fiber amplifier, only ~26% of the pump is absorbed, and the efficiency is consequently much lower (23%).

The reason for this difference in absorption is that the unsaturated pump absorption coefficient in the cladding of the phosphate fiber is 58 dB/m. Therefore, most of the pump power is absorbed in this 30 cm phosphate fiber, and the amplifier has a high efficiency. In contrast, the corresponding absorption coefficient for the silica fiber is 4.1 dB/m only. Furthermore, the silica fiber cannot be any longer than 40 cm before the onset of SBS. Therefore, and as can be seen in Fig. 2(b), these two limitations result in a pump absorption efficiency of 26% only


Fig. 3. Experimental $Yb^{3+}$-doped phosphate fiber amplifier.

in the 40-cm silica fiber, which explains its much lower output power.

It has been shown that the SBS gain coefficient of an LMA silica fiber can be reduced to $\sim 9 \times 10^{-12}$ m/W, i.e., a factor of 5.5, by designing the fiber such that the core acts as an acoustic antiguiding region, which forces the acoustic-mode energy to be located away from the core [24]. Since this reduction greatly improves the maximum power that can be extracted from a single-frequency silica fiber MOPA, it was interesting to repeat this comparison assuming that the silica fiber exhibits this reduced SBS gain coefficient. The resulting SBS threshold power curve is shown in Fig. 2(b) as the top orange dashed curve for the acoustic antiguiding silica fiber. The silica fiber MOPA produces a maximum power of 578 W with a 56% conversion efficiency before the onset of SBS. This is still 20% lower than the output power of the phosphate fiber (702 W). The efficiency of the phosphate fiber MOPA is also ~13% higher. This advantage of phosphate fibers would be further enhanced if the fiber loss was to be reduced to the current bulk loss value of 0.43 dB/m [25] (same maximum output power, but an efficiency increased to 83%). Also, note that the damage threshold intensity assumed for the phosphate fiber (0.65 GW/cm$^2$) is a conservative value, and could be increased by placing a coreless fiber end-cap or silica window at the output of the phosphate fiber [26]. The maximum output power of a single-mode phosphate fiber could then be further increased by applying the antiacoustic guiding principle to phosphate fibers, although its applicability to a phosphate–glass fiber made by the rod-in-tube technique needs to be demonstrated.

The origin of this expected superior performance of a truly single-mode phosphate fiber MOPA is again that: 1) the phosphate fiber can be much more heavily doped with $Yb^{3+}$ (~15 times); hence, it is shorter and 2) has a lower SBS gain coefficient. The downside of this increased efficiency, however, is increased thermal loading in the phosphate fiber, which leads to a higher fiber temperature. As discussed in subsequent sections, this problem is quite manageable.

## IV. Demonstration of High-Power Single-Mode Fiber Amplifier and Laser

### A. 16 W Single-Frequency Phosphate Fiber Amplifier

The experimental setup for the $Yb^{3+}$-doped phosphate fiber MOPA is shown in Fig. 3. The gain medium was a 74.5-cm length of single-mode double-clad phosphate fiber. The fiber, of the type shown in Fig. 1(a), had a 355 $\mu$m outer cladding, a 240 $\mu$m inner cladding with an NA of 0.445, and a 10 $\mu$m core diameter with an NA of 0.07. The core diameter and NA

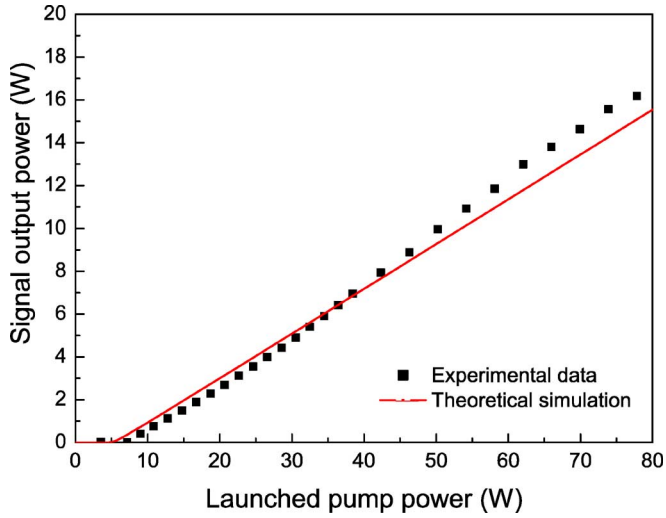


Fig. 4. Measured 1.03 $\mu$m signal output power generated by the 74.5 cm phosphate fiber amplifier as a function of launched pump power.

were designed to carry the fundamental mode only at wavelengths above 914 nm. The fiber core was uniformly doped with $1.42 \times 10^{21}$ $Yb^{3+}$/cm$^3$ (~12 wt% $Yb_2O_3$). Both fiber ends were polished at an 8° angle to prevent lasing. A counterpropagating geometry was chosen to maximize the amplifier output power. The fiber was pumped with a 972-nm fiber-coupled laser diode through a dichroic beam splitter placed on the signal output side. The fiber core was seeded with 31.6 mW of 1029.5 nm power from a commercial fiber laser with a full-width at half-maximum (FWHM) linewidth of less than 30 kHz. Both fiber ends were clamped in aluminum mounts. The pump-end mount was 10 in long and water-cooled to drain heat from the fiber-end region and prevent optical damage. The signal-end mount was served to drain heat passively from the end regions of the fiber. The reason for this asymmetry is that the thermal loading was much higher at the pump-end than at the signal-end.

The portion of fiber between the two mounts was also cooled by conduction by cementing it to a metal plate with a thin layer of UV glue to ensure good mechanical contact.

The measured output performance of this fiber MOPA is shown in Fig. 4. A maximum output power of 16.3 W, corresponding to a gain of 27 dB with respect to the launched signal power, was reached at an absorbed pump power of 28.1 W (76 W launched). To the best of our knowledge, this is the first report of a watt-level $Yb^{3+}$-doped phosphate fiber MOPA. The maximum output power was limited by the available pump power.

The solid curve in Fig. 4 was generated using the aforementioned numerical simulator and the measured fiber parameter values. The spatial overlap between the pump intensity distribution in the inner cladding and the dopant in the core has a strong influence on the rate of pump absorption along the fiber. Since this overlap is not known, we used it as a free fitting parameter to best match our code prediction to the experimental data points. The best-fit solid curve in Fig. 4 was obtained with a spatial overlap of 29.5%. (An overlap of 100% would correspond to

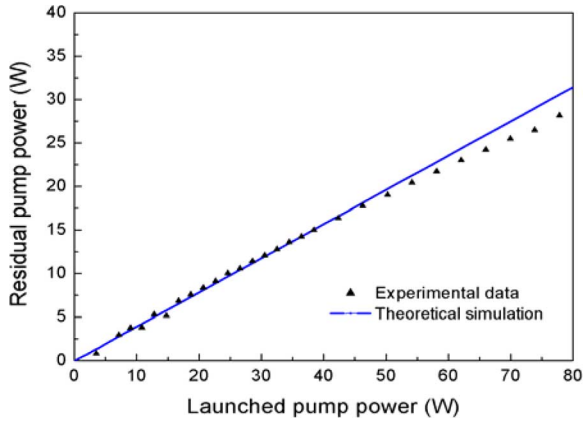


Fig. 5. Measured and simulated residual pump power as a function of launched pump power.

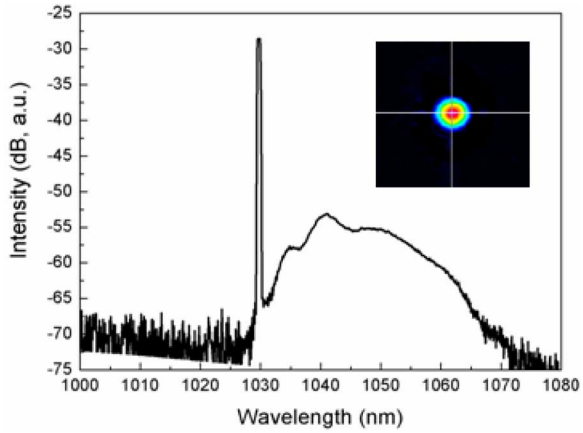


Fig. 6. Measured amplifier spectrum at an output power of 14.6 W. *The inset is the measured output beam profile*.

a pump distribution that is uniform across the core and inner cladding.) The theoretical curve agrees very well with the measured data. The slightly higher measured efficiency at higher pump powers is simply the result of the pump wavelength being red-shifted toward the 975-nm $Yb^{3+}$ absorption peak at higher diode drive currents.

The predicted 29.5% overlap was confirmed by studying the residual unabsorbed pump power transmitted by the fiber MOPA (see Fig. 3). Fig. 5 shows the measured unabsorbed pump power as a function of launched pump power. At the maximum launched pump power of 76 W, the unabsorbed pump power is as large as 28 W. Fig. 5 also shows the unabsorbed pump power predicted by the code for this amplifier, using the same parameter values as to generate the solid curve of Fig. 4, including a spatial overlap of 29.5%. The simulation curve matches the measured data well. This agreement confirms the numerical value of 29.5% for the pump/dopant overlap, and it explains why ~40% of the pump power was not absorbed in the fiber. This relatively low overlap is believed to be due to the high azimuthal symmetry of the core/inner cladding configuration that results in insufficient scattering of the pump modes in the fiber (which was kept straight). This overlap can be increased by using a fiber with an air hole parallel to the core [see Fig. 1(b)] [20], as demonstrated in the next section, or a polarization-maintaining fiber, where the stress rods then act as mode mixers.

The measured output spectrum of the fiber amplifier measured at 14.6 W is shown in Fig. 6. It indicates that the ASE power level is more than 25 dB below the 1029.5 nm signal level. The ratio of total ASE power to signal power was estimated as less than 1% from our code. As shown in the inset of Fig. 6, the output signal was in the fundamental fiber mode ($LP_{01}$) and of excellent quality, as expected for a step-index single-mode core.

### *B. 57-W Single-Mode Phosphate Fiber Laser*

Our early studies of phosphate fiber lasers taught us that adding an air hole to the inner cladding and making the core eccentric break the axial symmetry of the waveguide and greatly improve the pump/dopant spatial overlap [20]. It was therefore

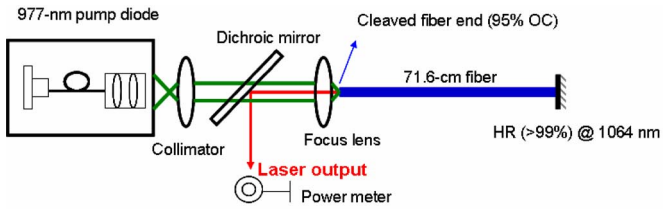


Fig. 7. Experimental $Yb^{3+}$-doped phosphate fiber laser.

interesting to test these air-hole fibers in our fiber MOPA. However, a high-gain fiber MOPA requires angled fiber ends to avoid lasing. We could neither polish the fiber ends (without clogging the air hole with debris that would induce optical damage) nor cleave them at an angle for lack of suitable equipment. As an alternative, to study the power scalability of this $Yb^{3+}$-doped phosphate fiber beyond the power level that we were able to achieve in an amplifier, we cleaved the ends of the fiber at 90° and used the fiber to make a phosphate fiber laser.

The experimental configuration of this laser is shown in Fig. 7. It consisted of a 71.6 cm length of air-hole $Yb^{3+}$-doped phosphate fiber placed in an optical cavity. One cavity mirror was a dielectric high reflector (HR) with a reflectivity greater than 99% at 1064 nm, butt coupled to one of the cleaved fiber ends. The other mirror was the other cleaved fiber end, which provided a 5% reflection and acted as the output coupler (OC). The cleaved fiber end is shown in Fig. 1(b). This fiber has the same structure as the fiber used in the fiber MOPA, except that the active core is offset from the fiber center and an air hole is added. The core and the air hole are symmetrically located with respect to the center of the fiber, and 30 $\mu$m apart center to the center. The fiber was cladding-pumped with a fiber-coupled laser diode at 977 nm through a dichroic beam splitter placed on the OC side. The fiber ends were cooled using the same arrangement as the MOPA, except that the 1-in mount at the mirror end was also water-cooled.

Our previous phosphate fiber laser [20] had a slope efficiency of 25.8%, which was limited by the relatively low absorption of the 940 nm pump. Significant efficiency improvement in the

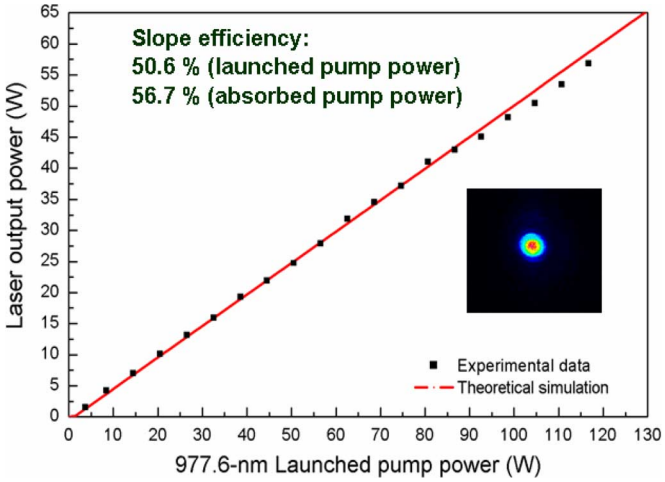


Fig. 8. 1.06 $\mu$m laser power generated by the 71.6 cm phosphate fiber laser as a function of the launched pump power at 977 nm. The inset shows the measured output beam profile.

same laser configuration was achieved by changing the pump wavelength to 977 nm, where $Yb^{3+}$ absorption is much stronger.

Fig. 8 shows the laser output power measured versus launched pump power. The threshold was ~3 W. The maximum output power was 56.9 W for 116.7 W of launched pump power (104.3 W absorbed). The output was in the $LP_{01}$ mode, and the laser FWHM linewidth was ~4 nm. The measured slope efficiency was 50.6% against launched pump power and 56.7% against absorbed pump power. These efficiencies are more than twice as high as in our previous laser [20]. In addition, these efficiencies are well predicted by our simulation if we assume a spatial overlap of 100% (solid curve in Fig. 8). At the maximum output power, we observed catastrophic damage of the fiber inside the pump-input V-groove mount near where the fiber exits the mount. We believe that the damage was likely caused by excessive stress applied to the fiber's outer surface by imperfections in the machined V-groove in which the fiber rested inside the mount, combined with the pump-induced increase in the fiber temperature.

The fiber length used in this laser was, in fact, optimized theoretically to maximize the laser output power at the highest available pump power. Although the slope efficiency is fairly good, it is not as high as could be, in spite of this optimization, because not all of the pump is absorbed, and further increasing the fiber length would increase the loss, at both the signal and pump, more than the gain. Simulations show that by reducing the fiber loss from 3 to 0.3 dB/m, the slope efficiency, after optimizing the length, would be as high as 86%, which is comparable to what is achievable in silica fibers. This analysis shows that it is crucial to study the origin of the loss in the phosphate fibers, in particular, whether it comes from absorption and scattering mechanisms. This information will provide useful hints as to what steps should be taken to reduce this loss. The fact that phosphate glass can be have a much lower loss (~0.43 dB/m) [25] than our current fibers suggests that this goal is achievable.

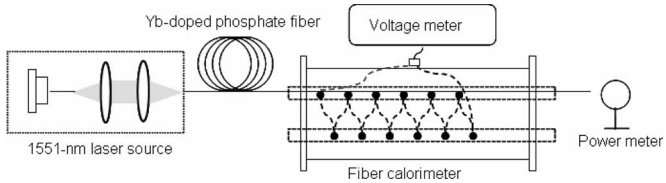


Fig. 9. Schematic diagram of the fiber calorimeter.

## V. Analysis of Fiber Loss

The propagation loss of our phosphate fibers is expected to arise primarily from absorption and/or scattering. Absorption converts light energy into heat that not only degrades the laser efficiency but also increases the fiber temperature. The lower efficiency results in a higher pump power requirement, which further increases the temperature. The higher temperature may result in thermal damage and limit the power scalability of the system. In contrast, if scattering is only a source of loss, it reduces efficiency without generating heat. We used this fundamental difference to measure these two components independently.

### A. Absorption Loss Measurements

In the absorption measurements, the fiber was placed in a calorimeter and optically probed with a 1.55 $\mu$m laser, where $Yb^{3+}$ does not absorb. Thermocouples inside the calorimeter measured the fiber temperature increase, from which, after suitable calibration, the amount of heat released by the fiber in the calorimeter per unit time could be calculated. As shown in Fig. 9, the calorimeter consisted of two identical glass capillaries placed inside a cylindrical aluminum shield [27]. The two capillary tubes were 16.2 cm long and had an inner diameter of 1 mm. The fiber under test was threaded through one capillary. The other capillary served as a reference. Six thermocouples were attached to both capillaries in series. They were evenly distributed along the capillaries so as to provide the temperature difference averaged over six points along the length of the capillaries. Because only temperature differences are measured, environmental temperature fluctuations are subtracted. The role of the aluminum shield was to maintain a homogeneous temperature distribution in the vicinity of the capillaries. The response of the calorimeter was calibrated by placing a copper wire with known resistance inside the capillary that normally receives the fiber, then sending a known current through it, giving us a known amount of heat.

A 119 cm length of unjacketed single-mode 12% Yb-doped phosphate fiber was used in this measurement. The fiber had a core diameter of 5 $\mu$m and a cladding diameter of 125 $\mu$m. Light from a 450 mW, 1551 nm laser pigtailed to a single-mode fiber was launched into the fiber core. Any light guided by the cladding was stripped carefully before the point of entry of the fiber into the calorimeter by placing index-matching gel on the fiber surface. Since the capillary' glass has negligible absorption around 1.55 $\mu$m, the portion of signal light scattered by the fiber was absorbed only by the aluminum shield, and thus, did not induce any heating of the capillaries. After turning on the

laser, the fiber temperature rose above the ambient temperature, from the absorbed power at 1551 nm, then quickly ($\sim$2 min) settled to a constant value. The absorption loss coefficient of the fiber was derived from the measured steady-state temperature difference between the capillaries and the measured transmitted laser power. The absorption loss coefficient obtained by this process is 2.27 dB/m.

### *B. Scattering Loss Measurements*

To cross check this absorption loss measurement, we also measured the scattering loss of a piece of fiber from the same spool. Portion of a 168 cm length of fiber was placed in 1-in-diameter integrating sphere coated with barium sulfate, and light from the 1551 nm laser was launched into the fiber. An InGaAs photodiode mounted in the output port of the integrating sphere measured the portion of fiber-guided laser light scattered in the sphere. A baffle was mounted parallel to the fiber to shield the detector from direct illumination with forward-scattered light. The fiber surface prior to its point of entry into the sphere was covered with index-matching gel to strip out cladding modes. The response of the integrating sphere was calibrated by pulling the fiber back until its free end was at the center of the sphere, then measuring the power collected by the detector and comparing it to the known power released inside the sphere. This procedure yielded a scattering coefficient of 0.68 dB/m.

The total loss of this fiber, measured by an independent cutback method, is 2.95 dB/m at 1551 nm. This value is in very good agreement with the sum of the measured absorption loss (2.27 dB/m) and scattering loss (0.68 dB/m) coefficients. The absorption loss, therefore, accounts for 77% of the total loss, and scattering for the remaining 23%. In principle, the absorption component is mainly due to impurities in source material, while scattering arises from inhomogeneities in the bulk and/or irregularities at the boundary between the core and inner cladding. This result (77%/23%) indicates that absorption loss must be reduced to improve the efficiency of the fiber laser.

## VI. Optical Damage Limit

The limitation that ultimately prevents further power scaling of any laser is optical damage caused by breakdown, thermal loading, or stress fracture. This limitation is anticipated to be more prominent in a soft glass such as a phosphate, compared, for example, to thermomechanically tougher glasses such as silica. To this end, it was interesting to study the thermal loading of our high-power phosphate fiber laser, and forecast how high a single-mode phosphate fiber laser can be scaled in power.

Three main optical damage mechanisms need to be assessed when dealing with CW lasers, namely: 1) optical surface damage arising from the high electric field at the input and output ends of the fiber; 2) melting of the glass; and 3) stress fractures caused by radial or longitudinal temperature gradients in the fiber. The surface damage threshold of a 10-$\mu$m single-mode phosphate fiber has been discussed in Section III. Melting and stress fracture in lasers are induced by excessive thermal loading of the laser material. Li *et al.* reported a 3-D thermal analysis of short-length phosphate fiber lasers [28]. Measurements have shown that when cooled with thermoelectric coolers (TECs), a fiber made with the same phosphate host as used in this paper exhibits no signs of damage at 1.5 $\mu$m at a thermal loading of 180 W/m. In addition, the thermal simulation further predicted that TEC-cooled phosphate fiber lasers have the potential to dissipate thermal loads up to $\sim$1 kW/m with the same cooling design. Assuming a weak dependence of damage on wavelength, this value can be used as a lower bound value for stress fracture and melting in a cooled $Yb^{3+}$-doped fiber source.

To evaluate how much power can be extracted from a $Yb^{3+}$-doped fiber laser source before this level of thermal loading is reached, we developed an analytical model of thermal loading. As in other hosts, in a pumped phosphate fiber, heat is produced first by the relaxation of phonons that make up for the quantum defect between the pump and laser photons, and second by the absorption component of the fiber loss that originates from impurities. Both the pump and the laser signal contribute to this second mechanism.

The heat generated per unit time $\Delta H_1$ by the first mechanism along a short length of fiber $\Delta z$ is given by

$$\Delta H_1(z) = \eta \alpha_{\mathrm{abs}}(z) P_p(z) \Delta z \tag{1}$$

where $\alpha_{\mathrm{abs}}(z)$ is the $z$-dependent, saturated absorption coefficient of $Yb^{3+}$ at the pump wavelength, $\eta$ is the quantum defect (only $\sim$8.9% in a 1064 nm laser pumped at 977 nm), and $P_p(z)$ is the remaining pump power at $z$.

The heat produced per unit time $\Delta H_2$ by absorption loss of the pump and signal along this same length of fiber $\Delta z$ is

$$\Delta H_2\,(z) = \alpha_a\,[P_p\,(z) + P_s\,(z)]\,\Delta z \tag{2}$$

where $\alpha_a$ is the absorption loss coefficient and $P_s(z)$ is the laser power at $z$. The total heat $\Delta H$ generated along the gain fiber, or thermal load, is the sum of these two contributions

$$\Delta H(z) = \Delta H_1(z) + \Delta H_2(z). \tag{3}$$

The thermal load of phosphate fiber lasers was evaluated numerically by making use of our simulator, which calculates, among many other parameters, the distribution of the signal and pump powers along the fiber. For simplicity, and without loss of accuracy, we assumed that the pump absorption loss is uniform across the core and inner cladding. The quantum-defect-induced loss is generated only inside the core.

Fig. 10 shows the thermal load calculated for the parameters of our experimental fiber laser at its maximum output power of 57 W. Both contributions, as well as the total thermal load, are plotted as a function of position along the fiber. All three curves decrease monotonically from the pumped (left) end of the fiber, as expected. The highest thermal loading is $\sim$200 W/m. The fiber loss accounts for more than 50% of the thermal loading, which stresses again the importance of reducing the fiber loss. If the absorption loss is removed, the loss contribution will become negligible, and the thermal loading will drop to $\sim$60 W/m, i.e., about 1 W/m per watt of output power, suggesting that from the standpoint of thermal loading and heat removal alone, at least $\sim$1 kW could be extracted from this truly single-mode device.

The shaded area in Fig. 10 identifies the portion of the pump-side fiber-end that was cooled actively. As mentioned earlier, at

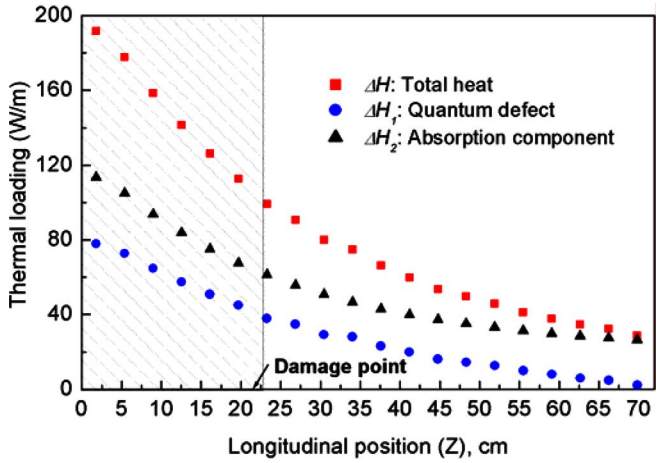


Fig. 10. Calculated thermal loading of the 56.9 W phosphate fiber laser.

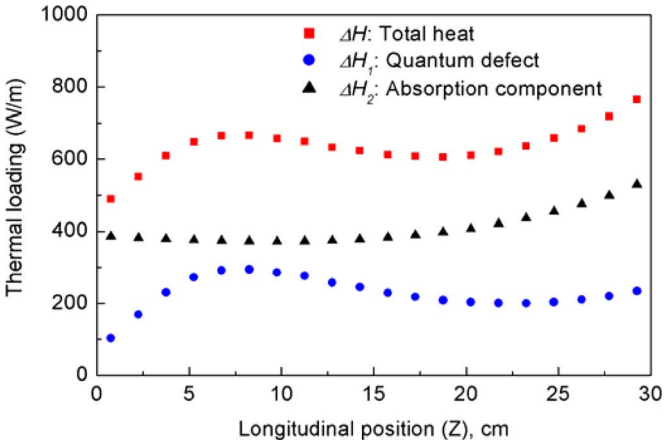


Fig. 11. Calculated thermal loading of the proposed 700 W phosphate fiber MOPA.

the highest pump power, the fiber damaged at the point identified by the arrow that is near the uncooled portion of the fiber. When replaced, the next fiber also damaged at about the same point. This seems to suggest that the damage was caused by an excessive longitudinal temperature gradient in this region as well as imperfections in the machined V-groove. Cooling the entire fiber should solve this problem.

In addition, we plot the calculated thermal loading for the 700 W phosphate fiber MOPA, reported in Section II-B, as shown in Fig. 11. The launched pump power was taken to be 700 W in the forward direction and 300 W in the backward direction. The fiber core diameter was 10 $\mu$m, the core NA 0.07, the inner cladding diameter 125 $\mu$m, and the pump wavelength 975 nm. The total pump power was selected to produce a maximum output of 700 W equal to the surface-damage threshold for this core size. Again, the loss contribution dominates. The thermal loading is more uniform because of bidirectional pumping. The maximum thermal loading is approximately constant and under 800 W/m. This simulation shows that the thermal-loading limit ($>$1 kW/m) is not reached before the onset of surface damage. With suitable cooling, the maximum output power of a single-mode $Yb^{3+}$-doped fiber laser can be limited by the ultimate damage mechanism, i.e., surface damage.

## VII. Conclusion

$Yb^{3+}$-doped phosphate fibers constitute a promising gain element for power-scaling truly single-mode single-frequency fiber amplifiers to near the kilowatt level. We have shown that as a result of their extremely high doping level, low SBS gain coefficient, and absence of photodarkening. Numerical simulations predict that in a double-clad, step-index phosphate fiber heavily doped with $Yb^{3+}$, up to $\sim$700 W of single-frequency single-mode power can be generated without the onset of SBS, at a thermal-loading level that can be handled by a cooled fiber. As a proof of principle, we report the first high-power sources in a $Yb^{3+}$-doped phosphate fiber, namely, a 1.03 $\mu$m fiber MOPA producing 16 W of single-frequency power and a 57 W multiple-frequency 1.03 $\mu$m fiber laser. Both sources used only $\sim$75 cm of a step-index single-mode fiber doped with as much as 12 wt% $Yb_2O_3$. The slope efficiency of these sources (51% and 57% with respect to absorbed and launched pump power, respectively) is found to be limited by the fairly high fiber loss ($\sim$3 dB/m). Measurements indicate that 77% of this loss is due to impurity absorption, and the rest to scattering. By reducing the fiber loss from 3 to 0.3 dB/m, the slope efficiency of these phosphate fiber lasers will be as high as 86%, and the thermal loading can be decreased by more than 3 dB. Further studies will focus on reducing this loss and developing cooling systems to achieve higher powers.

## Acknowledgment

The authors thank C. W. Rudy for assistance in the fiber scattering loss measurement.

## References

[1] V. Gapontsev, D. Gapontsev, N. Platonov, O. Shkurikh, V. Fomin, A. Mashkin, M. Abramov, and S. Ferin, "2 kW CW ytterbium fiber laser with record diffraction-limited brightness," in *Proc. Conf. Lasers Electro-Opt. Eur.*, Munich, Germany, Jun. 12–17, 2005, p. 508.

[2] Y. Jeong, J. Sahu, D. Payne, and J. Nilsson, "Ytterbium-doped large-core fiber laser with 1.36 kW continuous-wave output power," *Opt. Express*, vol. 12, no. 25, pp. 6088–6093, 2004.

[3] S. Gray, A. Liu, D. T. Walton, J. Wang, M.-J. Li, X. Chen, A. B. Ruffin, J. A. DeMeritt, and L. A. Zenteno, "502 watt, single transverse mode, narrow linewidth, bidirectionally pumped Yb-doped fiber amplifier," *Opt. Express*, vol. 15, no. 25, pp. 17044–17050, 2007.

[4] Y. Jeong, J. Nilsson, J. K. Sahu, D. N. Payne, L. M. B. Hickey, and P. W. Turner, "Power scaling of single-frequency ytterbium-doped fiber master-oscillator power-amplifier sources up to 500 W," *IEEE J. Quantum Electron.*, vol. 13, no. 3, pp. 546–549, May/Jun. 2007.

[5] E. Snitzer, H. Po, F. Hakimi, R. Tumminelli, and B. C. McCollum, "Double-clad, offset core Nd fiber laser," presented at the Opt. Fiber Sens. 1998, OSA Tech. Dig. Ser., Washington, DC, vol. 2, Paper PD5.

[6] Z. Burshtein, Y. Kalisky, S. Z. Levy, P. Le Boulanger, and S. Rotman, "Impurity local phonon nonradiative quenching of $Yb^{3+}$ fluorescence in Ytterbium-doped silicate glasses," *IEEE J. Quantum Electron.*, vol. 26, no. 8, pp. 1000–1007, Aug. 2000.

[7] Y.-W. Lee, S. Sinha, M. J. F. Digonnet, R. L. Byer, and S. Jiang, "Measurement of high photodarkening resistance in heavily $Yb^{3+}$-doped phosphate fibers $Yb^{3+}$-doped phosphate fiber laser," *Electron. Lett.*, vol. 44, no. 1, pp. 14–16, 2008.

[8] M. E. Fermann, "Single-mode excitation of multimode fibers with ultrashort pulses," *Opt. Lett.*, vol. 23, no. 1, pp. 52–54, 1998.

[9] J. W. Nicholson, A. D. Yablon, S. Ramachandran, and S. Ghalmi, "Spatially and spectrally resolved imaging of modal content in large-mode-area fibers," *Opt. Express*, vol. 16, no. 10, pp. 7233–7243, 2008.
[10] B. Willke, N. Uehara, E. K. Gustafson, R. L. Byer, P. J. King, S. U. Seel, and R. L. Savage, Jr., "Spatial and temporal filtering of a 10-W Nd:YAG laser with a Fabry–Perot ring-cavity premode cleaner," *Opt. Lett.*, vol. 23, no. 21, pp. 1704–1706, 1998.
[11] Y.-W. Lee, K. E. Urbanek, M. J. F. Digonnet, R. L. Byer, and S. Jiang, "Measurement of the stimulated Brillouin scattering gain coefficient of a phosphate fiber," *Proc. SPIE*, vol. 6469, p. 64690L, 2007.
[12] R. Paschotta, J. Nilsson, A. Tropper, and D. C. Hanna, "Ytterbium-doped fiber amplifiers," *IEEE J. Quantum Electron.*, vol. 33, no. 7, pp. 1049–1056, Jul. 1997.
[13] NP Photonics, Tuscon, AZ, unpublished.
[14] S. Suzuki1, S. Jiang, N. Peyghambarian, and A. Chavez-Pirson, "Image amplifier based on $Yb^{3+}$ -doped multi-core phosphate optical fiber," *Opt. Express*, vol. 15, no. 7, pp. 3759–3765, 2007.
[15] E. Snitzer and R. Tumminelli, "SiO2-clad fibers with selectively volatilized soft-glass cores," *Opt. Lett.*, vol. 14, no. 14, pp. 757–759, 1989.
[16] T. Qiu, L. Li, A. Schulagen, V. L. Temyanko, T. Luo, S. Jiang, A. Mafi, J. V. Moloney, and N. Peyghambarian, "Generation of 9.3-W multimode and 4-W single-mode output from 7-cm short fiber lasers," *IEEE Photon. Technol. Lett.*, vol. 16, no. 12, pp. 2592–2594, Dec. 2004.
[17] J. L. Wagener, D. G. Falquier, M. J. F. Digonnet, and H. J. Shaw, "A Mueller matrix formalism for modeling polarization effects in Erbium-doped fiber," *J. Lightw. Technol.*, vol. 16, no. 2, pp. 200–206, Feb. 1998.
[18] D. G. Falquier, J. L. Wagener, M. J. F. Digonnet, and H. J. Shaw, "Polarized superfluorescent fiber sources," *Opt. Fiber Technol.*, vol. 4, no. 4, pp. 453–470, 1998.
[19] S. Sinha, "Power scaling long-wavelength $Yb^{3+}$ -doped silica fiber lasers for frequency doubling to yellow," Ph.D. dissertation, Stanford Univ., Stanford, CA, ch. 2, pp. 57–70.
[20] Y.-W. Lee, S. Sinha, M. J. F. Digonnet, R. L. Byer, and S. Jiang, "20 W single-mode $Yb^{3+}$ -doped phosphate fiber laser," *Opt. Lett.*, vol. 31, no. 22, pp. 3255–3257, 2006.
[21] J. Koponen, M. Söderlund, H. J. Hoffman, D. A. V. Kliner, and J. P. Koplow, "Photodarkening measurements in large mode area fibers," *Proc. SPIE*, vol. 6453, p. 64531E, 2007.
[22] J. Limpert, F. Roser, S. Klingebiel, T. Schreiber, C. Wirth, T. Pesche, R. Eberhardt, and A. Tunnermannl, "The rising power of fiber lasers and amplifiers," *IEEE J. Sel. Topics Quantum Electron.*, vol. 13, no. 3, pp. 537–545, May/Jun. 2007.
[23] J. H. Campbell and T. I. Suratwala, "Nd-doped phosphate glasses for high-energy/high-peak-power lasers," *J. Non-Cryst. Solids*, vol. 263/264, pp. 318–341, 2000.
[24] M.-J. Li, X. Chen, J. Wang, S. Gray, A. Liu, J. A. Demeritt, A. B. Ruffin, A. M. Crowley, D. T. Walton, and L. A. Zenteno, "Al/Ge co-doped large mode area fiber with high SBS threshold," *Opt. Express*, vol. 15, no. 13, pp. 8290–8299, 2007.
[25] F. Hanson and G. Imthurn, "Efficient laser diode side pumped neodymium glass slab laser," *IEEE J. Quantum Electron.*, vol. QE-24, no. 9, pp. 1811–1813, Sep. 1988.
[26] S. Sinha, K. E. Urbanek, A. Krzywicki, and R. L. Byer, "Investigation of the suitability of silicate bonding for facet termination in active fiber devices," *Opt. Express*, vol. 15, no. 20, pp. 13003–13022, 2007.
[27] D. H. Jundt, "Lithium niobate: Single crystal fiber growth and quasi-phase-matching," Ph.D. dissertation, Stanford Univ., Stanford, CA, 1991, pp. A77–A83.
[28] L. Li, H. Li, T. Qiu, V. L. Temyanko, M. M. Morrell, and A. Schülzgen, "3-Dimensional thermal analysis and active cooling of short-length high-power fiber lasers," *Opt. Express*, vol. 13, no. 59, pp. 3420–3428, 2005.

**Yin-Wen Lee** received the B.S. degree in atomic science and the M.S. degree in electrical engineering from National Tsinghua University, Hsinchu, Taiwan, in 1998 and 2000, respectively. She is currently working toward the Ph.D. degree in applied physics at Stanford University, Stanford, CA.

Her current research interests include high-power fiber lasers and amplifiers, with special focus on power scaling capabilities of Yb-doped phosphate fibers.

Ms. Lee is a member of the Optical Society of America (OSA) and the International Society for Optical Engineering (SPIE).

**Michel J. F. Digonnet** (M'01) received the degree in engineering from Ecole Supérieure de Physique et de Chimie de la Ville de Paris, Paris, France, the Diplome d'Etudes Approfondies in coherent optics from the University of Paris, Paris, in 1978, and the M.S. and Ph.D. degrees from the Applied Physics Department, Stanford University, Stanford, CA, in 1980 and 1983, respectively.

His doctoral research centered on wavelength-division multiplexing (WDM) fiber couplers and single-crystal fibers. From 1983 to 1986, he was a Visiting Scholar at Stanford University, where he was engaged in conducting research on miniature solid-state sources and integrated optics for fiber sensors. From 1986 to 1990, he was involved in the development of dye and 2 $\mu$m solid-state lasers, fiber sensors, and fiber delivery systems for laser angioplasty with MCM Laboratories, Mountain View, CA. He is currently a Senior Research Associate in the Department of Applied Physics, Stanford University, where he teaches a course entitled lasers, as well as short courses on fiber amplifiers and lasers and fiber sensors at international conferences. He has authored or coauthored 190 articles, held nearly 60 patents, edited several books, and chaired numerous conferences on optical fiber devices, sensors, and materials. His current research interests include photonic bandgap fibers, fiber sensors, and sensor arrays, high-power ceramic lasers, fiber lasers and amplifiers, fiber gratings, slow light, and optical microcavities.

**Supriyo Sinha** received the B.A.Sc. degree in computer engineering with physics from the University of Waterloo, Waterloo, ON, Canada, in 2000, and the M.S. and Ph.D. degrees in electrical engineering from Stanford University, Stanford, CA, in 2002 and 2007, respectively.

His doctoral research centered on long-wavelength ytterbium fiber lasers and amplifiers and low-noise high-power single-frequency fiber systems. In 2007, he was a Postdoctoral Scholar in Professor Byer's Research Group, where he was engaged in research on ultrafast fiber lasers and silicate bonding. Since 2008, he has been an Optical Engineer at Raydiance, Inc. Los Altos, CA, where he is engaged in research on ultrafast fiber systems.

Dr. Sinha is a member of the Optical Society of America (OSA).

**Karel E. Urbanek** received the B.S. degree in applied physics and the B.A. degree in economics from the University of California, Davis, in 1997, and the M.Sc. degree in applied physics from Stanford University, Stanford, CA, in 2003.

From 1997 to 2000, he was initially a Technician and later an Engineering Technician with Spectra-Physics, where he was engaged in gaining experience with gas, solid state, and ultrafast lasers. In 1996, he spent the summer working on rebuilding a COIL system at the National Science Institute, Prague, Czech Republic. Since 2003, he has been a Physical Sciences Research Assistant in the Byer and Fejer Research Groups, Stanford University. His current research interests include high-power fiber amplifiers, low-noise single-frequency sources, solid-state amplifiers, and nonlinear frequency conversion for use in near-IR and visible laser systems.

**Robert L. Byer** (M'75–M'83–F'87) received the Ph.D. degree in applied physics from Stanford University, Stanford, CA, in 1969.

He is a Professor of Applied Physics at Stanford University, Stanford, CA, where he has conducted research and taught classes in lasers and nonlinear optics since 1969. He was the Chair of the Applied Physics Department from 1981 to 1984, the Associate Dean of Humanities and Sciences from 1985 to 1987, and the Vice Provost and Dean of Research from 1987 to 1992. From 1997 to 2006, he was the Director of Hansen Experimental Physics Laboratory. From 2006 to 2008, he was the Director of Edward L. Ginzton Laboratory. He has made numerous contributions to laser science and technology including the demonstration of the first tunable visible parametric oscillator, the development of the Q-switched unstable resonator Nd:YAG laser, remote sensing using tunable IR sources, and precision spectroscopy using coherent anti-Stokes Raman scattering. He has authored or coauthored more than 500 scientific papers and holds 50 patents in the fields of lasers and nonlinear optics. His current research interests include the development of advanced nonlinear optical materials and laser-diode-pumped solid-state laser sources for application to gravitational wave detection and laser particle acceleration.

Prof. Byer is a Fellow of the Optical Society of America, the American Physical Society, and the American Association for the Advancement of Science. In 1985, he was the President of the IEEE Lasers and Electro-Optics Society, and in 1994, the President of the Optical Society of America. From 1995 to 1998, he was the Chair of the California Council on Science and Technology, of which he is a Founding Member. He has served on the Engineering Advisory Board of the National Science Foundation. In 1996, he received the Quantum Electronics Award from the IEEE Lasers and Electro-Optics Society. In 1998, he received the Schawlow Award of the Laser Institute of America and the R. W. Wood Prize of the Optical Society of America. He was elected to the National Academy of Engineering in 1987.

**Shibin Jiang** received the Ph.D. degree from the Universite de Rennes 1, Rennes, France, in 1996.

He is currently the President of AdValue Photonics, Inc, Tucson, AZ, and also an Adjunct Research Professor in the College of Optical Sciences, University of Arizona, Tucson, where he was an Assistant Research Professor. He was the Chief Technology Officer and the Co-Founder of NP Photonics, Inc., Tucson. His current research interests include innovative glasses and fibers, high power fiber lasers and amplifiers, mode-locked fiber lasers, THz source generation, low noise single frequency fiber lasers, tunable lasers, and fiber sensor systems. He authored/co-authored 60 peer-reviewed journal publications, edited 12 proceedings books, and was awarded 23 US patents in the area of photonic glass materials and devices.

Dr. Jiang is the recipient of the 2005 Gottardi Prize from International Commission on Glass. He is a Fellow of the International Society for Optical Engineering (SPIE) and the American Ceramic Society.